Electronic and magnetic properties of superconducting LnO1−xFxBiS2 (Ln = La, Ce, Pr, and Nd) from first principles

Corentin Morice, Emilio Artacho, Siân E. Dutton, Hyeong-Jin Kim, Siddharth S. Saxena

Angaben zur Veröffentlichung / Publication details:

Morice, Corentin, Emilio Artacho, Siân E. Dutton, Hyeong-Jin Kim, and Siddharth S. Saxena. 2016. "Electronic and magnetic properties of superconducting LnO1−xFxBiS2 (Ln = La, Ce, Pr, and Nd) from first principles." *Journal of Physics: Condensed Matter* 28 (34): 345504. https://doi.org/10.1088/0953-8984/28/34/345504.

Journal of Physics: Condensed Matter

PAPER • OPEN ACCESS

Electronic and magnetic properties of superconducting $LnO_{1-x}F_xBiS_2$ (Ln = La, Ce, Pr, and Nd) from first principles

To cite this article: Corentin Morice *et al* 2016 *J. Phys.: Condens. Matter* **28** 345504

OPEN ACCESS
IOP Publishing
Journal of Physics: Condensed Matter
J. Phys.: Condens. Matter **28** (2016) 345504 (10pp)
doi:10.1088/0953-8984/28/34/345504

Electronic and magnetic properties of superconducting $LnO_{1-x}F_xBiS_2$ (Ln = La, Ce, Pr, and Nd) from first principles

Corentin Morice[1], Emilio Artacho[1,2,3], Siân E Dutton[1], Hyeong-Jin Kim[1] and Siddharth S Saxena[1]

[1] Cavendish Laboratory, University of Cambridge, Cambridge CB3 0HE, UK
[2] Nanogune and DIPC, Tolosa Hiribidea 76, 20018 San Sebastián, Spain
[3] Basque Foundation for Science, Ikerbasque, 48011 Bilbao, Spain

E-mail: cm712@cam.ac.uk, ea245@cam.ac.uk and sss21@cam.ac.uk

Received 1 April 2016, revised 31 May 2016
Accepted for publication 1 June 2016
Published 29 June 2016

Abstract

A density functional theory study of the BiS_2 superconductors containing rare-earths: $LnO_{1-x}F_xBiS_2$ (Ln = La, Ce, Pr, and Nd) is presented. We find that $CeO_{0.5}F_{0.5}BiS_2$ has competing ferromagnetic and weak antiferromagnetic tendencies, the first one corresponding to experimental results. We show that $PrO_{0.5}F_{0.5}BiS_2$ has a strong tendency for magnetic order, which can be ferromagnetic or antiferromagnetic depending on subtle differences in 4*f* orbital occupations. We demonstrate that $NdO_{0.5}F_{0.5}BiS_2$ has a stable magnetic ground state with weak tendency to order. Finally, we show that the change of rare earth does not affect the Fermi surface, and predict that $CeOBiS_2$ should display a pressure induced phase transition to a metallic, if not superconducting, phase under pressure.

Keywords: superconductivity, BiS_2-based, DFT, *ab initio*

S Online supplementary data available from stacks.iop.org/JPhysCM/28/345504/mmedia

(Some figures may appear in colour only in the online journal)

1. Introduction

The excitement generated by the recent finding of two new superconductors, $Bi_3O_2S_3$ and $LaO_{1-x}F_xBiS_2$ [1, 2], led to the unveiling of a whole class of superconductors containing BiS_2 bilayers. These compounds share a common two-dimensional structure with alternating BiS_2 bilayers and spacer layers. It is the BiS planes in the BiS_2 bilayers which are thought to be responsible for superconductivity in these compounds [3]. Soon after the discovery of superconductivity in $LaO_{1-x}F_xBiS_2$, chemical substitution to tune the properties was attempted. The first research axis was to replace the lanthanum atom by other lanthanides: cerium, praseodymium, neodymium, europium and ytterbium [4–12]. Hole and electron doping of the parent compound has also been studied in $Sr_xLa_{1-x}FBiS_2$ [13] and $La_{1-x}M_xOBiS_2$ (M = Ti, Zr, Hf, Th) [14, 15] respectively.

The electronic and thermodynamic properties of this group of materials are indeed interesting and theoretical suggestions for the mechanism of superconductivity range from spin-fluctuation mediated superconductivity [16], to proximity to ferroelectricity and charge density wave (CDW) instabilities [17, 18]. Recent work even revealed the potential of related materials for photovoltaic applications [19]. Ferromagnetism has been shown experimentally to coexist with superconductivity in $CeO_{0.5}F_{0.5}BiS_2$ [7, 20–27], and

quantum critical fluctuations of the magnetic moments have been observed in $CeOBiS_2$ [28].

The electronic structure of the two first compounds to be found, $Bi_3O_2S_3$ [3] and $La(O,F)BiS_2$ [17, 29–31], was calculated. These calculations indicated that the superconducting electrons are a mixture of Bismuth 6 $p_{x,\,y}$ and Sulphur 3 $p_{x,\,y}$ states [29, 30]. These form eight bands, four of which are under the Fermi level, when the other four either are above the Fermi level or cross it.

The coupling mechanism for superconductivity has been investigated in various ways. Electron–phonon interactions have been calculated in $La(O,F)BiS_2$, and yield a large electron–phonon coupling constant, suggesting superconductivity in this compound is strongly coupled and conventional [17, 18, 32]. Renormalisation-group calculations suggested triplet pairing and weak topological superconductivity [33, 34], a possibility studied in the context of quasiparticle interference [35]. Random phase approximation was applied to a two-orbital model [30], leading to an extended s-wave or d-wave pairing [16, 36].

In this paper we present our findings from electronic structure calculations for the stoichiometric and doped series of materials $LnO_{1-x}F_xBiS_2$ with $Ln =$ La, Ce, Pr and Nd, and $x = 0$, 0.5. The doped phases calculated have been reported as being superconducting, and the parent phases have been reported as being non-superconducting.

We first show that the change of rare earth does not affect the Fermi surface and that the conduction electrons are confined to the bismuth-sulphur planes. We then demonstrate that $CeO_{0.5}F_{0.5}BiS_2$ has competing ferromagnetic and weak antiferromagnetic tendencies. The ferromagnetic tendency is in agreement with experimental results. We show that $PrO_{0.5}F_{0.5}BiS_2$ has a strong tendency to magnetic order, which could be ferromagnetic or antiferromagnetic depending on subtle differences in 4*f* orbital occupations. We show that $NdO_{0.5}F_{0.5}BiS_2$ has a stable weakly antiferromagnetic ground state. Finally, we predict that applying pressure to $CeOBiS_2$ would make it metallic, and possibly superconducting.

2. Methods

We limit our study to materials which crystal structure has been experimentally determined, with the exception of the Ce doped compound. We have been able to provide a structure through relaxation methods for the Ce compound, since the availability of the La, Pr and Nd compounds provides a reasonable reliability on the starting point.

Band structures and densities of states were calculated within density functional theory using the SIESTA method [38, 39], implementing the generalized gradient approximation (GGA) in the shape of the Perdew, Burke, and Ernzerhof functional [40] and the GGA+U method. It uses norm-conserving pseudopotentials to replace the core electrons, while the valence electrons are described using atomic-like orbitals as basis states at the double zeta polarized level. These pseudopotentials include scalar relativistic corrections. Spin–orbit coupling was not included but has been shown in previous work to be of no relevance to the main features at the Fermi level in this family of materials [3, 18]. Details on the basis sets used are available in the supplemental material (stacks.iop.org/JPhysCM/28/345504/mmedia).

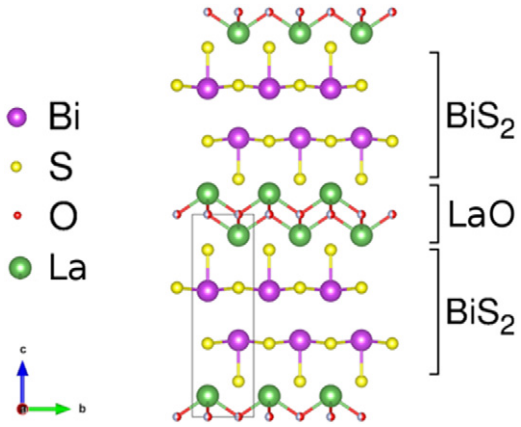

Figure 1. Crystal structure of $LaOBiS_2$, represented in VESTA [37]. All the compounds studied share this same structure, with replacement of lanthanum by other lanthanides, or of oxygen by fluorine. The black solid line represents the unit cell, which contains two formula units.

Calculations for $x = 0.5$ have been performed for all the compounds. All these structures share the same space group: P4/nmm (figure 1). The calculations for the lanthanum compound were performed without spin polarisation. However for $Ln \neq$ La, the presence of unpaired 4*f* electrons demands the use of spin polarisation in the calculations. Calculations for the La compound were performed using experimental data for the geometry obtained after high pressure treatment of the sample, for which the maximal superconducting T_c (10.6 K) was found [1]. For the Pr and Nd compounds, we used structural experimental data for the systems for which T_c of 5.5 K [5] and 5 K were found [6] respectively.

No atomic coordinates have been reported for the Ce compound yet, so we obtained a geometry from density functional theory (DFT) by relaxing the structure (both atoms and cell), starting from the structure known for the La compound. Two relaxations were performed, one with a *k*-grid of $8 \times 8 \times 3$ points, a standard set of parameters and without U, and one with a *k*-grid of $15 \times 15 \times 5$ points, a high quality set of parameters and with $+U$. Both relaxations were performed in the ferromagnetic configuration. The comparison of the results shows the relaxation is well converged: the lattice constants differ by approximately 2 mÅ, and the fractional atomic coordinates by less than 0.0004. The details of the crystal structures are available in the supplementary material. The obtained atomic positions and a lattice parameter are very close to the ones of the Pr doped compound. The c lattice parameter is significantly smaller than the ones of the other doped compounds. This is in accordance with mismatches between DFT and experiments in the inter-layer forces noted in other compounds of this family of superconductors [3].

There are two O/F sites in each unit cell of every doped compound. It has been shown that disorder in the O and F positions has a very minor effect on the electronic structure at the level discussed in this work [41]. As already done in

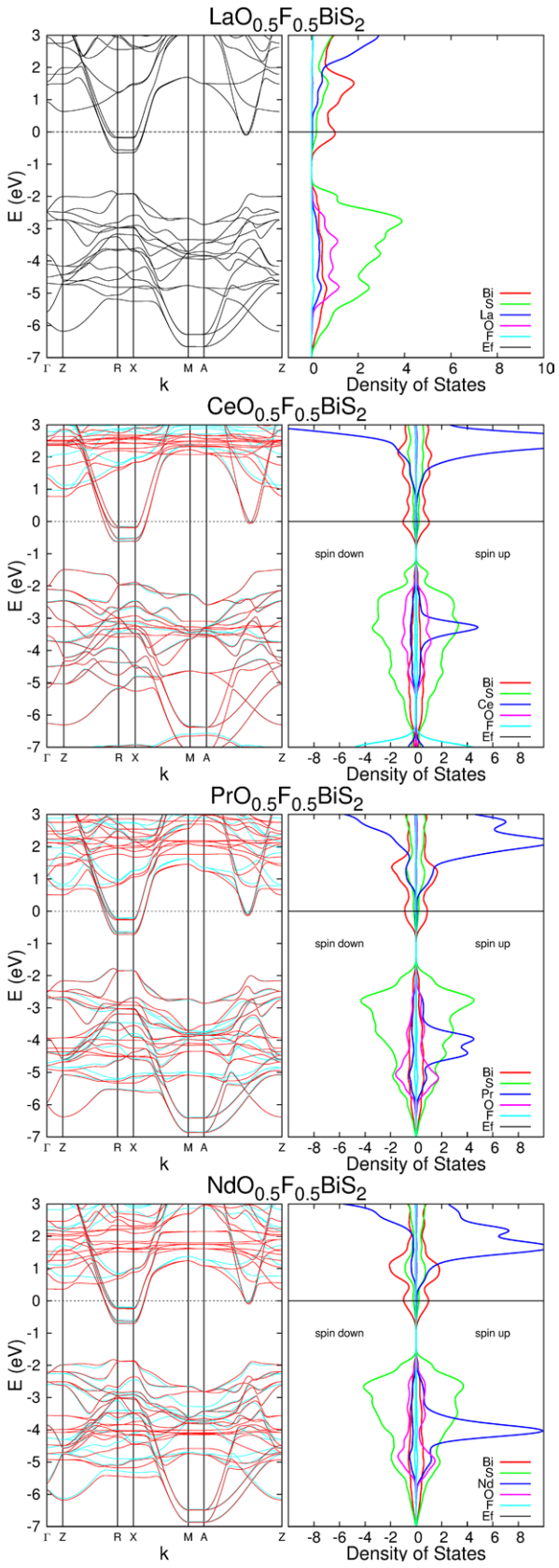

Figure 2. Band structures (left) and densities of states projected onto the basis orbitals for Bi (red), S (green), *Ln* (blue), O (lilac), and F (light blue) (right) for the four doped compounds. For the three compositions having 4*f* electrons, we use $U = 5$. The lanthanum compound band structure is non spin polarised, whereas the other three are spin polarised, in the ferromagnetic configuration.

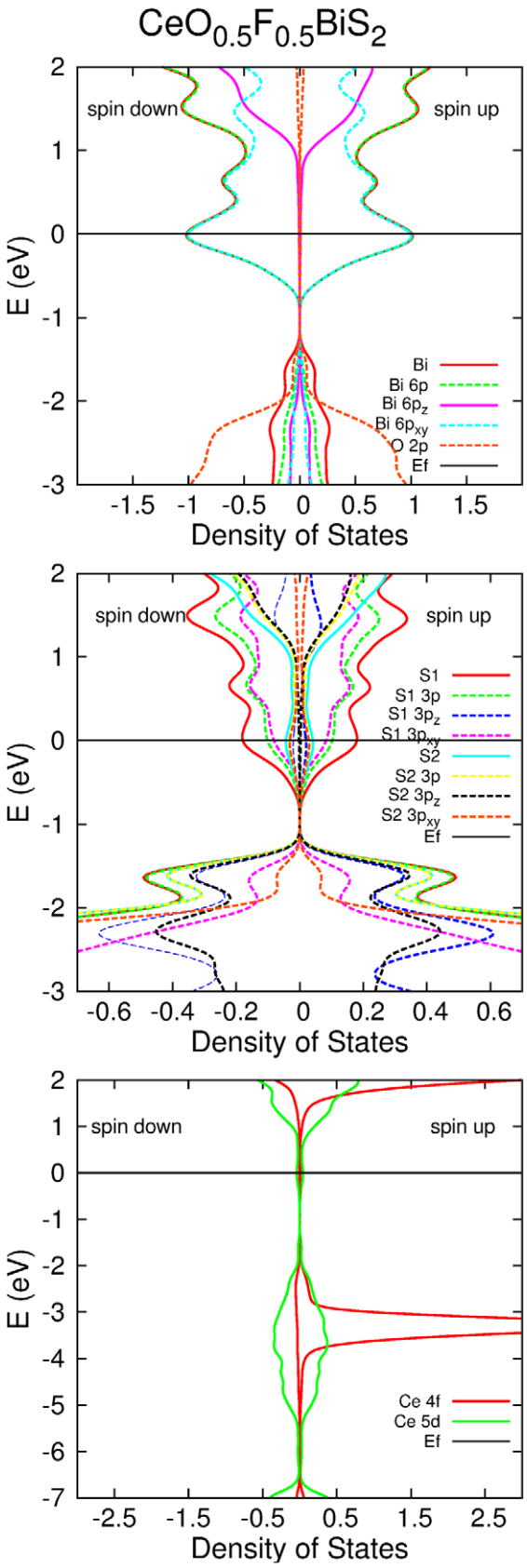

Figure 3. Densities of states in $CeO_{0.5}F_{0.5}BiS_2$, projected onto several basis orbitals. S1 stands for the in-plane sulphur atom, and S2 stands for the out-of-plane sulphur atom. The label p_{xy} is a shorthand for p_x and p_y orbitals which have the same density of states. We use $U = 5$ and spin polarisation.

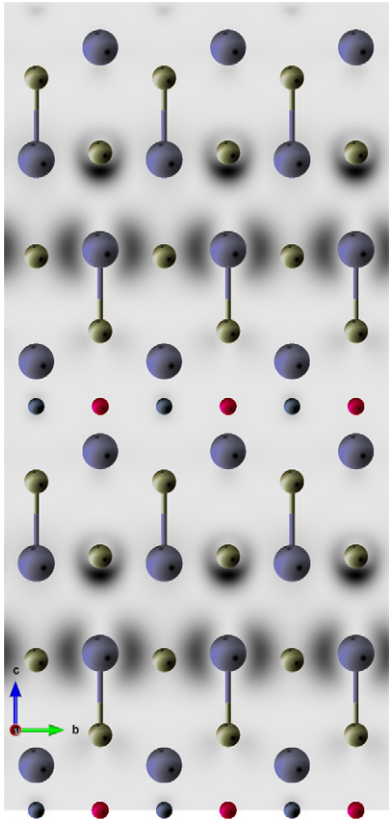

Figure 4. Local density of states of $CeO_{0.5}F_{0.5}BiS_2$ in real space integrated in the energy range [−0.5,0], plotted with XCrySDen [49]. Half of the atoms represented are not in the plane corresponding to the density plot: the atoms in the unit cell are arranged on two planes parallel to the *x*-*z* plane. The density plot corresponds to only one of these two planes. The BiS planes (horizontal and perpendicular to the figure) gather the vast majority of the density.

Table 1. Orbitals occupied by the 4*f* electron in each cerium atom in the unit cell of $CeO_{0.5}F_{0.5}BiS_2$ in the two antiferromagnetic configurations AF1 and AF2.

	4*f* occupations	
Configuration	1st Ce atom	2nd Ce atom
F	$4f_{5yz^2-yr^2}$	$4f_{5yz^2-xr^2}$
AF1	$4f_{5yz^2-yr^2}$	$4f_{5yz^2-xr^2}$
AF2	$4f_{y^3-3x^2y}$	$4f_{5yz^2-xr^2}$

Note: The labelling order of the cerium atoms is arbitrary.

[17, 29, 31], we assign O to (0,0,0) and F to (0.5,0.5,0) in the La doped compound and O to (0.75,0.25,0) and F to (0.25,0.75,0) in the other doped compounds. This changes the space group of the crystal structures of the doped compounds to $P\bar{4}m2$.

We also performed calculations on two parent phases: $LaOBiS_2$ and $CeOBiS_2$. Their space group is also P4/nmm. We used experimental structural data for both [42, 43], and performed spin-polarised calculations in the ferromagnetic configuration for $CeOBiS_2$. There are no experimental data available for the other two parent compounds to our knowledge.

Table 2. Total energies of the various magnetic configurations obtained for $CeO_{0.5}F_{0.5}BiS_2$ with respect to the energy of F.

Configuration	Total energy (eV)
F	0
AF1	−0.0124
AF2	0.1105

We performed GGA + *U* calculations [44] for all the compounds except the lanthanum ones, because of the known strong correlation of the 4*f* electrons in cerium, praseodymium and neodymium. The current implementation of DFT + *U* in SIESTA is based on the formulation by Dudarev *et al* [45] which combines the two parameters *U* and *J* to produce an effective Coulomb repulsion $U_{\text{eff}} = U - J$ which we call *U* in the following. The double-counting scheme used is also the one described by Dudarev *et al* [45]. Given the intrinsic difficulty in the *ab initio* determination of a value of *U* [46], we explored the behaviour of the system for *U* varying from 3 to 7 eV. The influence of *U* on relaxations was investigated and proven to be negligible. Here we discuss results obtained with $U = 5$ eV, given that this value is standard for the atoms we are dealing with [47, 48]. We tested the robustness of the results for *U* between 3 eV and 7 eV.

Monkhorst–Pack sampling of the Brillouin zone was used for all calculations. *k*-point sampling proved to be quite delicate, and large sets were used to obtain reasonably converged results, especially for the convergence of magnetic results. The grids used were $25 \times 25 \times 8$ for the Ce and Nd compounds, $35 \times 35 \times 11$ for the Pr compound and $24 \times 24 \times 5$ for the La compound. The band structure results converged for lower sets, and the results in figure 6 were obtained for $8 \times 8 \times 3$ sets.

3. Results

3.1. Band structures

We calculated the band structure of the four doped compounds. We observe many similarities between them, due to their proximity in terms of composition and crystal structure (figure 2). More precisely, we find the same four bands (or eight bands with spin polarisation) near the R and X points, and two (or four) bands near the middle of the A–Z segment close to the Fermi level in all the compounds. They are similar to the ones in the Bi-O-S compounds [3]. They are crossing the Fermi level for the doped compounds, and lie above the Fermi level for the two parent phases. The projected densities of states indicate that these bands are formed from Bi and S states. It has already been shown in $Bi_3O_2S_3$ and in the La compound that the main contribution to these bands comes from Bi 6*p* states and S 3*p* states. It is confirmed in all the systems considered here, as figure 3 shows. There we plotted the results for $CeO_{0.5}F_{0.5}BiS_2$, these being similar in all the compounds considered. The position of the Fermi level with respect to the bottom of these bands is very similar in all the compounds with

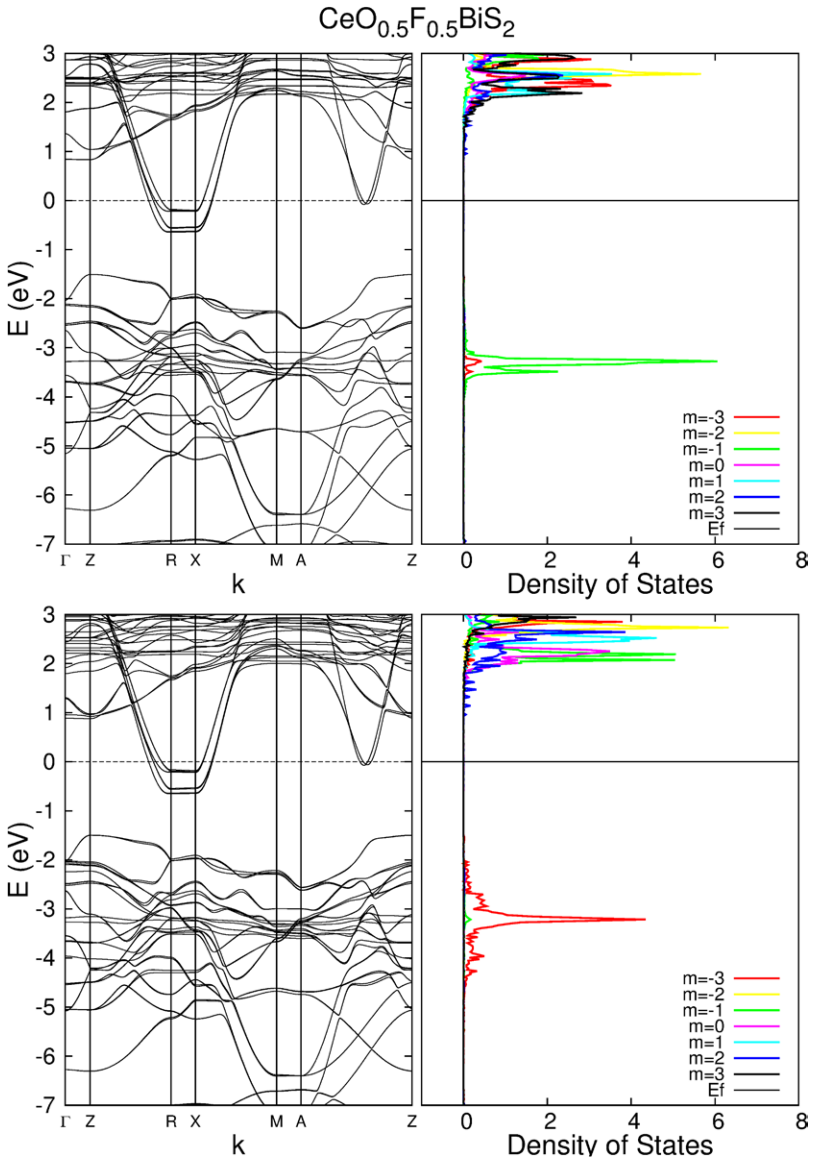

Figure 5. Band structures and density of 4*f* states of $CeO_{0.5}F_{0.5}BiS_2$ in the antiferromagnetic configuration, in the two states that it converges to. The projected densities of states were plotted using a peak width of 0.01 eV, smaller than the standard 0.2 eV used in the rest of this work. State AF1 is at the top, and state AF2 at the bottom. The decomposition of density of states on the 9 orbitals clearly shows that the two configurations differ by the jump of one electron from one orbital to another.

$x = 0.5$. The main effect of the fluorine doping is a shift of the Fermi level, as reported previously [29–31].

To explore further the character of the bands just below the Fermi level, we plotted the local density of states (LDOS) resolved in real space for the $x = 0.5$ compounds for energies integrated between −0.5 eV and 0 eV (figure 4). The results confirm what had been found in other BiS_2-based compound: all these electrons accumulate around the BiS planes [3]. This can also be seen in the partial density of states at the Fermi level (figure 3) which is very low for the out-of-plane sulphur atoms. This raises the question of the existence of superconductors that have BiS planes without BiS_2 layers. Some p_z participation is involved in the slight puckering of the BiS planes, inducing a clear distortion (along z) of the LDOS.

The lanthanide bands are at least 3 eV below and 0.5 eV above the Fermi level. The Fermi surface is robust to lanthanide substitution and to the change of U between 3 eV and 7 eV. There is no difference in the density of states at the Fermi energy between compounds, the lanthanides' bands being far from the Fermi level, as expected, because of the strong correlation of the 4*f* electrons. The extra electrons remain in the lanthanide bands and away from the Fermi level, hence the change of lanthanide has almost no effect. The Fermi surface is almost identical in the four cases, and does not seem to be responsible for the substantial change observed in T_c, nor does the band structure as a whole.

3.2. Magnetic order

We considered the magnetic properties of the doped compounds. They each have two *Ln* atoms per unit cell. We compared the total energies of the ferromagnetic configuration,

Table 3. Orbitals occupied by the 4*f* electron in each praseodymium atom in the unit cell of $PrO_{0.5}F_{0.5}BiS_2$ in the four configurations FM1, FM2, AF1 and AF2.

	4*f* occupations			
	1st Pr atom		2nd Pr atom	
Configuration	1st electron	2nd electron	1st electron	2nd electron
F1	$4f_{5yz^2-yr^2}$	$4f_{5yz^2-xr^2}$ and $4f_{x^3-3xy^2}$	$4f_{5yz^2-xr^2}$	$4f_{5yz^2-yr^2}$ and $4f_{y^3-3x^2y}$
F2	$4f_{xyz}$	$4f_{5yz^2-yr^2}$ and $4f_{y^3-3x^2y}$	$4f_{5yz^2-xr^2}$	$4f_{5yz^2-yr^2}$ and $4f_{y^3-3x^2y}$
AF1	$4f_{xyz}$	$4f_{5yz^2-xr^2}$ and $4f_{x^3-3xy^2}$	$4f_{xyz}$	$4f_{5yz^2-xr^2}$ and $4f_{x^3-3xy^2}$
AF2	$4f_{xyz}$	$4f_{5yz^2-xr^2}$ and $4f_{x^3-3xy^2}$	$4f_{5yz^2-xr^2}$	$4f_{5yz^2-yr^2}$ and $4f_{y^3-3x^2y}$

Note: The labelling order of the praseodymium atoms and electrons is arbitrary.

Table 4. Total energies of the various magnetic configurations obtained for $PrO_{0.5}F_{0.5}BiS_2$ with respect to the total energy of F1.

Configuration	Total energy (eV)
F1	0
F2	0.094527
AF1	0.092904
AF2	−0.000248

where the spins of the two atoms are aligned, and of the only antiferromagnetic configuration available in one unit cell, where the spins of the two atoms are antialigned.

Bulk cerium, praseodymium and neodymium have respectively one, three and four 4*f* electrons per atom. The two-electrons difference between Ce and Pr is due to the fact that bulk cerium has one electron in a 5*d* band, whereas bulk praseodymium and neodymium have not. However when we place these elements in the compounds considered here, each atom of these species has one 5*d* electron, thereby restoring the sequence. As expected the 4*f* electrons are polarised and the 5*d* are not. The spin polarisation $N_{\text{up}} - N_{\text{down}}$ is therefore 1, 2 and 3 electrons for the Ce, Pr and Nd atoms in their respective compounds. The 5*d* electron is unpolarised and strongly hybridised with other bands (figure 3).

These compounds share the space group P4/nmm. The lanthanide atoms are on the sites (1/4,1/4,*z*) and (3/4,3/4,− *z*). These have a 4mm symmetry. Hence the sites have the point group C_{4v}. The nearest neighbours of the lanthanide atoms are 4 oxygen atoms. As a way of characterising the 4*f* orbitals in this environment, we treat the *Ln* and the 4 O atoms as a molecule and look for the symmetries of the molecular orbitals for bonding in that molecule. Finally, we obtain that all the 4*f* orbitals are allowed by symmetry to hybridise with the oxygen atoms, except the $4f_{zx^2-zy^2}$ orbital, but it is never occupied, see below.

3.2.1. $CeO_{0.5}F_{0.5}BiS_2$. In the cerium compound we find two different competing states which are quasi-degenerate in energy. It does not make sense for us to try to establish which one is favoured since either state appears in the calculations under very slight changes of the technical parameters, even for very tightly converged settings (see the methods section).

In the ferromagnetic configuration, calculations always converge on the same state which we call state F. But in the antiferromagnetic configuration, calculations converge on two different states, state AF1 and state AF2. They differ by the 4*f* orbital chosen by the 4*f* electrons in the Ce atoms. The orbital occupations of the 4*f* electron are summarised in table 1. The total energy of state AF2 is higher than the one of state F, while the total energy of state AF1 is lower than the one of state F (table 2). Therefore we obtain two competing states, F and AF1.

In state AF1 the spin–spin interaction is weak, with a slight tendency for them to order antiferromagnetically, as manifested by the energy difference with respect to ferromagnetic order of 12 meV per cell. In state F the ferromagnetic order is more substantially favoured, by 111 meV per cell.

The band structures and density of states for states AF1 and AF2 are plotted in figure 5. The bands are very similar, and quite indistinguishable around the Fermi level. The only difference is that in state AF2 the bands around the peak in 4*f* density of states are slightly higher than in state AF1. However, the projected density of states on the different *f*-orbitals clearly show the change of orbital character of the 4*f* electron.

The ferromagnetic state is compatible with experimental observations of ferromagnetism in this compound at low temperature. The presence of the weak antiferromagnetic state suggests that this system may be close to an antiferromagnetic instability associated to a change of orbital for the 4*f* electron, which would suggest possibly interesting phenomena associated with this coupling between spin ordering and choice of orbital.

3.2.2. $PrO_{0.5}F_{0.5}BiS_2$. A similar instability is observed in the Pr compound, in which each praseodymium atom has two electrons in the 4*f* shell. We obtain an effective degeneracy between two states for both the ferromagnetic (states F1 and F2) and the antiferromagnetic (states AF1 and AF2) configurations. In all cases the spin polarisation is 2 electrons on each atom. The two states on which each configuration converges only differ by the orbital occupations of the 4*f* electrons of the praseodymium atoms. The orbital occupations of the 4*f* electron are summarised in table 3.

For the same input parameters we obtain either F1 and AF1 or F2 and AF2. Therefore for a given set of parameters we obtain two energy differences, AF1-F1 and AF2-F2. These are 92.9 meV in favor of ferromagnetism and 94.8 meV in favor of antiferromagnetism, hence we obtain two competing states, AF2 and F1 (table 4).

The Pr compound has therefore two competing states, with very close energies. Both display magnetic ordering, with a

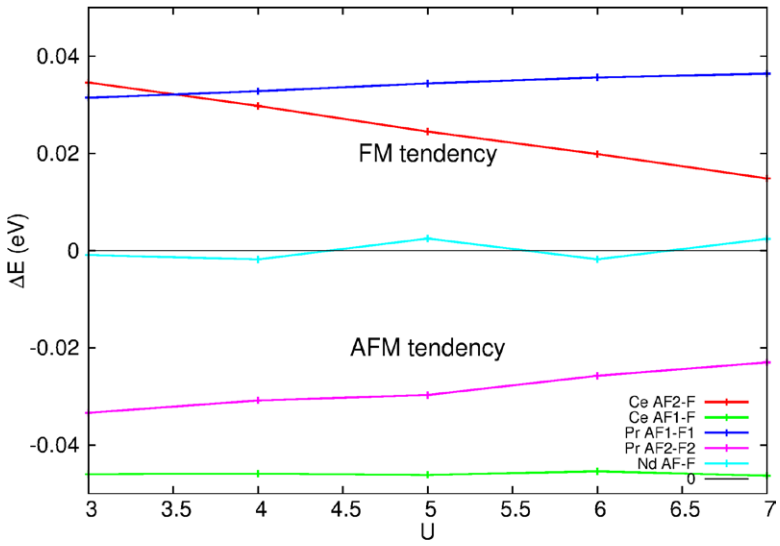

Figure 6. Difference of total energy per unit cell of $LnO_{0.5}F_{0.5}BiS_2$ (Ln = Ce, Pr, Nd) between antiferromagnetic state and ferromagnetic states, for U varying between 3 and 7. The k-point sampling set used here is smaller than in the rest of the text (see the methods section). The key is labelled with names of magnetic configurations defined in the main text. A positive difference means the tendency is ferromagnetic.

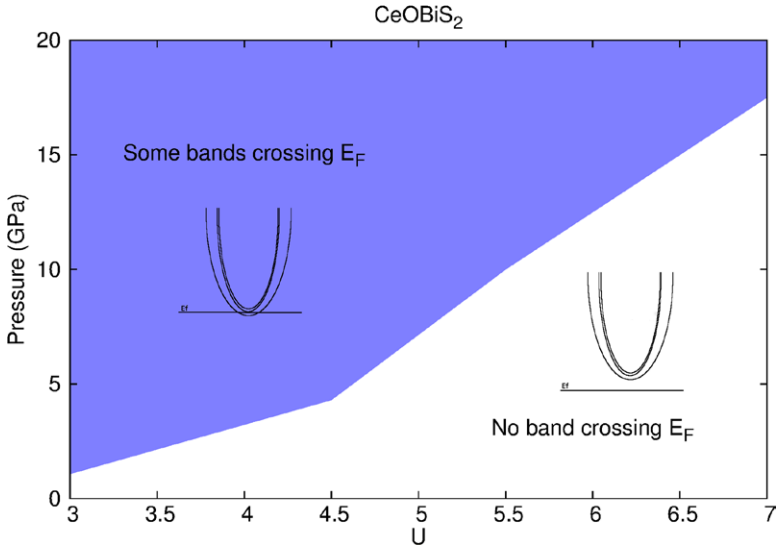

Figure 7. Pressure / U phase diagram of $CeOBiS_2$.

strength very close to the one in $CeO_{0.5}F_{0.5}BiS_2$, one ferromagnetic and the other antiferromagnetic.

3.2.3. $NdO_{0.5}F_{0.5}BiS_2$. In this case we find a single ferromagnetic state and a single antiferromagnetic one. We obtain a difference between the two spin states of 3.3 meV favouring antiferromagnetic order. This is very small, indeed it is two orders of magnitude lower than the difference in favor of ferromagnetism in the cerium compound. It is therefore likely that the magnetic order in this material will arise at temperatures much lower than the Curie temperature of the order of 1 K measured in the cerium compound.

The presence of an instability in the cerium and praseodymium doped compounds is consistent with the well known valence fluctuation phenomenon which has been studied in other compounds containing these two atoms [50, 51]. To the knowledge of the authors, no neodymium compound exhibits this phenomenon, which is in line with its absence in $NdO_{0.5}F_{0.5}BiS_2$.

The results discussed above for the three compounds do not change qualitatively with the choice of U value, as shown in figure 6, where the energy difference between the antiferromagnetic and the ferromagnetic configurations are shown for the three compounds. Calculating the total energy of other magnetic configurations using a larger unit cell has been attempted but definite conclusions could not be achieved, partly because of the described instabilities.

3.3. $CeOBiS_2$ under pressure

Finally, we consider the effect of pressure on $CeOBiS_2$. Without electron doping the system is insulating with the BiS

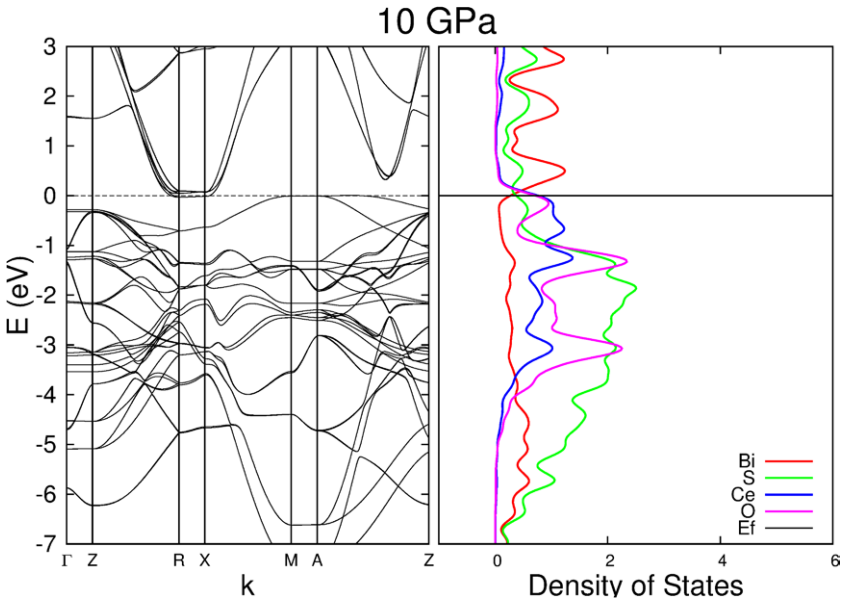

Figure 8. Band structure (left) and density of states projected onto the basis orbitals for Bi (red), S (green), Ce (blue), and O (lilac) (right) for $CeOBiS_2$ under 10 GPa. We use $U = 5$ and spin polarisation.

bands clearly above the Fermi level. The question is whether pressure can close that gap. The band structure of $CeOBiS_2$ has been calculated with respect to pressure and U (figures 7 and 8). At ambient pressure, the system is insulating. When pressure increases, the gap closes and some band cross the Fermi level. The transition pressure varies with U, from 1.2 GPa for $U = 3$ eV to 17.5 GPa for $U = 7$ eV. The bands crossing the Fermi level are not only the BiS bands: other bands are crossing. These are cerium bands, hybridised with oxygen and sulphur bands. Indeed, the main effect of pressure is to raise the cerium oxide bands which in turn dope the BiS bands. This effect is similar to the stoichiometric doping of the BiS bands by the sulphur dimers bands in $Bi_3O_2S_3$ [3]. The contribution of the oxygen and sulphur bands decreases with pressure but remains substantial, as can be seen in the density of states. The composition of the BiS bands does not change with pressure, it is always dominated by the same Bi 6*p* and S 3*p* states. Finally, the conduction band is narrowed whereas the valence band is slightly widened with pressure. Detailed plots of the band structures and densities of states, and crystal structures obtained are available in the supplementary material.

The insulating state at ambient pressure is consistent with the fact that no superconductivity has been observed in this compound. It shows that there should be a insulator-metal transition under pressure, which also could be superconducting at low temperature. The transition pressures obtained have rather large uncertainties given that they have been obtained through DFT-GGA (with its well-known bad gap problem), but we can still conclude that it seems likely the transition temperature could be reachable by commonly known techniques. Of course, this pressure also depends heavily on the U parameter relevant for the compound.

The type of 'doping' involved is different from the fluorine type. Indeed, here pressure brings the valence and the conduction bands together until they cross. Pressure has opposite effects on the valence and conduction bands: the conduction band is narrowed and its composition does not change, whereas the valence band is widened and its hybridisation with oxygen and sulphur orbitals is decreased.

4. Conclusion

We calculated the band structure of the four doped compounds and showed that the change of rare earth does not affect the Fermi surface. We calculated the local density of states, which clearly indicates that the conduction electrons are confined to the bismuth-sulphur planes.

We calculated the difference in energy between the two possible magnetic configurations one can obtain in one unit cell of $LnO_{1-x}F_xBiS_2$ (Ln = Ce, Pr, and Nd). We demonstrated that $CeO_{0.5}F_{0.5}BiS_2$ has competing ferromagnetic and weak antiferromagnetic tendencies. The first case corresponds to experimental results. $PrO_{0.5}F_{0.5}BiS_2$ has a strong tendency to order, which could be ferromagnetically or antiferromagnetically depending on subtle differences in 4*f* orbital occupations. $NdO_{0.5}F_{0.5}BiS_2$ has a stable weakly antiferromagnetic competing state.

Finally, we did predict that applying pressure to $CeOBiS_2$ would make it metallic, and possibly superconducting, through raising the cerium oxide bands. This type of doping of the BiS bands has not been investigated in the BiS_2 family so far and could have novel properties.

Acknowledgments

We would like to thank Arman Khojakhmetov for his exploratory work, and Gilbert G Lonzarich, Peter Littlewood, Pablo Aguado Puente, Stephen Rowley, Sebastian Haines, Cheng Liu, Daniel Molnar and Adrien Amigues for fruitful discussions. We acknowledge computing resources of the Spanish

Supercomputer Network (RES), and support from EPSRC, Corpus Christi College, and the Winton Programme for the Physics of Sustainability.

References

[1] Mizuguchi Y, Demura S, Deguchi K, Takano Y, Fujihisa H, Gotoh Y, Izawa H and Miura O 2012 Superconductivity in novel BiS_2-based layered superconductor $LaO_{1-x}F_xBiS_2$ *J. Phys. Soc. Japan* **81** 114725

[2] Mizuguchi Y, Fujihisa H, Gotoh Y, Suzuki K, Usui H, Kuroki K, Demura S, Takano Y, Izawa H and Miura O 2012 BiS_2-based layered superconductor $Bi_4O_4S_3$ *Phys. Rev.* B **86** 220510

[3] Morice C, Artacho E, Dutton S E, Molnar D, Kim H-J and Saxena S S 2015 Effects of stoichiometric doping in superconducting Bi-O-S systems *J. Phys.: Condens. Matter* **27** 135501

[4] Demura S *et al* 2013 New member of BiS_2-based superconductor $NdO_{1-x}F_xBiS_2$ *J. Phys. Soc. Japan* **82** 033708

[5] Jha R, Kumar A, Singh S K and Awana V P S 2013 Synthesis and superconductivity of new BiS_2 based superconductor $PrO_{0.5}F_{0.5}BiS_2$ *J. Supercond. Novel Magn.* **26** 499–502

[6] Jha R, Kumar A, Singh S K and Awana V P S 2013 Superconductivity at 5 K in $NdO_{0.5}F_{0.5}BiS_2$ *J. Appl. Phys.* **113** 056102

[7] Xing J, Li S, Ding X, Yang H and Wen H-H 2012 Superconductivity appears in the vicinity of semiconducting-like behavior in $CeO_{1-x}F_xBiS_2$ *Phys. Rev.* B **86** 214518

[8] Suzuki K, Tanaka M, Denholme S J, Fujioka M, Yamaguchi T, Takeya H and Takano Y 2015 Pressure-induced superconductivity in BiS_2-based $EuFBiS_2$ *J. Phys. Soc. Japan* **84** 115003

[9] Guo C Y *et al* 2015 Evidence for two distinct superconducting phases in $EuBiS_2F$ under pressure *Phys. Rev.* B **91** 214512

[10] Zhai H-F *et al* 2014 Possible charge-density wave, superconductivity, and *f*-electron valence instability in $EuBiS_2F$ *Phys. Rev.* B **90** 064518

[11] Goto Y, Kajitani J, Mizuguchi Y, Kamihara Y and Matoba M 2015 Electrical and thermal transport of layered bismuth-sulfide $EuBiS_2F$ at temperatures between 300 and 623 K *J. Phys. Soc. Japan* **84** 085003

[12] Yazici D, Huang K, White B D, Chang A H, Friedman A J and Maple M B 2013 Superconductivity of F-substituted $LnOBiS_2$ (Ln = La, Ce, Pr, Nd, Yb) compounds *Phil. Mag.* **93** 673–80

[13] Lin X *et al* 2013 Superconductivity induced by La doping in $Sr_{1-x}La_xFBiS_2$ *Phys. Rev.* B **87** 020504

[14] Yazici D, Huang K, White B D, Jeon I, Burnett V W, Friedman A J, Lum I K, Nallaiyan M, Spagna S and Maple M B 2013 Superconductivity induced by electron doping in $La_{1-x}M_xOBiS_2$ (M = Ti, Zr, Hf, Th) *Phys. Rev.* B **87** 174512

[15] Benayad N, Djermouni M and Zaoui A 2014 Electronic structure of new superconductor $La_0.5Th_0.5OBiS_2$: {DFT} study *Comput. Condens. Matter* **1** 19–25

[16] Martins G B, Moreo A and Dagotto E 2013 RPA analysis of a two-orbital model for the BiS_2-based superconductors *Phys. Rev.* B **87** 081102

[17] Yildirim T 2013 Ferroelectric soft phonons, charge density wave instability and strong electron–phonon coupling in BiS_2 layered superconductors: a first-principles study *Phys. Rev.* B **87** 020506

[18] Wan X, Ding H-C, Savrasov S Y and Duan C-G 2013 Electron–phonon superconductivity near charge-density-wave instability in $LaO_{1-x}F_xBiS_2$: density-functional calculations *Phys. Rev.* B **87** 115124

[19] Meng S, Zhang X, Zhang G, Wang Y, Zhang H and Huang F 2015 Synthesis, crystal structure, and photoelectric properties of a new layered bismuth oxysulfide *Inorg. Chem.* **54** 5768–73

[20] Jha R and Awana V P S 2013 Superconductivity in layered $CeO_{0.5}F_{0.5}BiS_2$ *J. Supercond. Novel Magn.* **27** 1–4

[21] Demura S *et al* 2015 Coexistence of bulk superconductivity and magnetism in $CeO_{1x}F_xBiS_2$ *J. Phys. Soc. Japan* **84** 024709

[22] Kajitani J, Hiroi T, Omachi A, Miura O and Mizuguchi Y 2015 Increase in T_c and change of crystal structure by high-pressure annealing in BiS_2-based superconductor $CeO_0.3F_0.7BiS_2$ *J. Supercond. Novel Magn.* **28** 1129–33

[23] Lee J *et al* 2014 Coexistence of ferromagnetism and superconductivity in $CeO_{0.3}F_{0.7}BiS_2$ *Phys. Rev.* B **90** 224410

[24] Miura A, Nagao M, Takei T, Watauchi S, Mizuguchi Y, Takano Y, Tanaka I and Kumada N 2015 Structure, superconductivity, and magnetism of $Ce(O,F)BiS_2$ single crystals *Cryst. Growth Des.* **15** 39–44

[25] Paris E, Joseph B, Iadecola A, Sugimoto T, Olivi L, Demura S, Mizuguchi Y, Takano Y, Mizokawa T and Saini N L 2014 Determination of local atomic displacements in $CeO_1xF_xBiS_2$ system *J. Phys.: Condens. Matter* **26** 435701

[26] Sugimoto T, Joseph B, Paris E, Iadecola A, Mizokawa T, Demura S, Mizuguchi Y, Takano Y and Saini N L 2014 Role of the Ce valence in the coexistence of superconductivity and ferromagnetism of $CeO_{1-x}F_xBiS_2$ revealed by Ce L_3-edge x-ray absorption spectroscopy *Phys. Rev.* B **89** 201117

[27] Sugimoto T *et al* 2015 Fermi surfaces and orbital polarization in superconducting $CeO_{0.5}F_{0.5}BiS_2$ revealed by angle-resolved photoemission spectroscopy *Phys. Rev.* B **92** 041113

[28] Higashinaka R, Asano T, Nakashima T, Fushiya K, Mizuguchi Y, Miura O, Matsuda T D and Aoki Y 2015 Pronounced log T divergence in specific heat of nonmetallic $CeOBiS_2$: a mother phase of BiS_2-based superconductor *J. Phys. Soc. Japan* **84** 023702

[29] Shein I R and Ivanovskii A L 2013 Electronic band structure and fermi surface for new layered superconductor $LaO_{0.5}F_{0.5}BiS_2$ in comparison with parent phase $LaOBiS_2$ from first principles *JETP Lett.* **96** 769–74

[30] Usui H, Suzuki K and Kuroki K 2012 Minimal electronic models for superconducting BiS_2 layers *Phys. Rev.* B **86** 220501

[31] Suzuki K, Usui H and Kuroki K 2013 Minimum model and its theoretical analysis for superconducting materials with BiS_2 layers *Phys. Procedia* **45** 21–4 (*Proc. of the 25th Int. Symp. on Superconductivity*)

[32] Li B, Xing Z W and Huang G Q 2013 Phonon spectra and superconductivity of the BiS_2-based compounds $LaO_{1-x}F_xBiS_2$ *Europhys. Lett.* **101** 47002

[33] Yao H and Yang F 2013 Topological odd-parity superconductivity at type-II 2D Van Hove singularities *Phys. Rev.* B **92** 035132

[34] Yang Y, Wang W-S, Xiang Y-Y, Li Z-Z and Wang Q-H 2013 Triplet pairing and possible weak topological superconductivity in BiS_2-based superconductors *Phys. Rev.* B **88** 094519

[35] Gao Y, Zhou T, Huang H, Tong P and Wang Q-H 2014 Testing the $d^*_{x^2-y^2}$-wave pairing symmetry by quasiparticle interference and knight shift in BiS_2-based superconductors *Phys. Rev.* B **90** 054518

[36] Zhou T and Wang Z D 2013 Probing the superconducting pairing symmetry from spin excitations in BiS_2 based superconductors *J. Supercond. Novel Magn.* **26** 2735–40
[37] Momma K and Izumi F 2011 *VESTA3* for three-dimensional visualization of crystal, volumetric and morphology data *J. Appl. Crystallogr.* **44** 1272–6
[38] Artacho E *et al* 2008 The SIESTA method; developments and applicability *J. Phys.: Condens. Matter* **20** 064208
[39] Soler J M, Artacho E, Gale J D, Garcia A, Junquera J, Ordejon P and Sanchez-Portal D 2002 The SIESTA method for *ab initio* order- n materials simulation *J. Phys.: Condens. Matter* **14** 2745
[40] Perdew J P, Burke K and Ernzerhof M 1996 Generalized gradient approximation made simple *Phys. Rev. Lett.* **77** 3865–8
[41] Lee J, Stone M B, Huq A, Yildirim T, Ehlers G, Mizuguchi Y, Miura O, Takano Y, Deguchi K, Demura S and Lee S-H 2013 Crystal structure, lattice vibrations, and superconductivity of $LaO_{1-x}F_xBiS_2$ *Phys. Rev.* B **87** 205134
[42] Tanryverdiev V S and Aliev O M 1995 *Int. J. Inorg. Mater.* **31** 1361
[43] Céolin R and Rodier N 1976 Structure cristalline de l'oxysulfure de cérium et de bismuth $CeBiOS_2$ *Acta Crystallogr.* B **32** 1476–9
[44] Anisimov V I, Zaanen J and Andersen O K 1991 Band theory and mott insulators: Hubbard *U* instead of stoner *I Phys. Rev.* B **44** 943–54
[45] Dudarev S L, Botton G A, Savrasov S Y, Humphreys C J and Sutton A P 1998 Electron-energy-loss spectra and the structural stability of nickel oxide: an LSDA + U study *Phys. Rev.* B **57** 1505–9
[46] Loschen C, Carrasco J, Neyman K M and Illas F 2007 First-principles LDA + U and GGA + U study of cerium oxides: dependence on the effective u parameter *Phys. Rev.* B **75** 035115
[47] Jiang H, Gomez-Abal R I, Rinke P and Scheffler M 2009 Localized and itinerant states in lanthanide oxides united by LDA *Phys. Rev. Lett.* **102** 126403
[48] Yeriskin I and Nolan M 2010 Doping of ceria surfaces with lanthanum: a DFT + U study *J. Phys.: Condens. Matter* **22** 135004
[49] Kokalj A 2003 Computer graphics and graphical user interfaces as tools in simulations of matter at the atomic scale *Comput. Mater. Sci.* **28** 155–68
[50] Holmes A T, Jaccard D and Miyake K 2007 Valence instability and superconductivity in heavy fermion systems *J. Phys. Soc. Japan* **76** 051002
[51] Herrero-Martín J *et al* 2011 Valence change of praseodymium in $Pr_{0.5}Ca_{0.5}CoO_3$ investigated by x-ray absorption spectroscopy *Phys. Rev.* B **84** 115131